

Rupture of an adjacent cerebral aneurysm following the deployment of a Pipeline embolization device: illustrative case

Atsushi Nakayashiki, MD,¹ Hiroyuki Sakata, MD, PhD,¹ Masayuki Ezura, MD, PhD,¹ Hidenori Endo, MD, PhD,¹ Takashi Inoue, MD, PhD,¹ Atsushi Saito, MD, PhD,¹ and Teiji Tominaga, MD, PhD²

¹Department of Neurosurgery, National Hospital Organization Sendai Medical Center, Sendai, Miyagi, Japan; and ²Department of Neurosurgery, Tohoku University Graduate School of Medicine, Sendai, Miyagi, Japan

BACKGROUND Although the Pipeline embolization device (PED) is effective for intracranial aneurysm treatment, its impact on the surrounding vascular structure is unknown.

OBSERVATIONS A 71-year-old woman was incidentally found to have a simultaneous large posterior communicating artery aneurysm and an ipsilateral small anterior choroidal artery aneurysm. She underwent flow diversion therapy for both aneurysms with a PED, but the distal shortening of the PED after deployment led to the exposure of the anterior choroidal artery aneurysm. Follow-up angiography revealed complete obliteration of the posterior communicating artery aneurysm, but the anterior choroidal artery aneurysm remained. Three years after the endovascular surgery, the patient experienced a subarachnoid hemorrhage due to the rupture of the anterior choroidal artery aneurysm. Retrospective analysis of angiographic images revealed a change in the vascular geometry surrounding the ruptured aneurysm after PED deployment; this was further accompanied by an increase in the flow velocity inside the aneurysm.

LESSONS Because PED use might induce the adverse effects on the adjacent uncovered aneurysm by changing the vascular geometry and hemodynamic stress, a cautious therapeutic strategy, such as proper placement of the stent and using a longer and appropriate-sized PED, should be chosen when deploying the PED.

<https://thejns.org/doi/abs/10.3171/CASE21651>

KEYWORDS Pipeline embolization device; device shortening; geometric change; hemodynamic change; subarachnoid hemorrhage

The Pipeline embolization device (PED; Covidien) is clinically effective for the treatment of unruptured intracranial aneurysms;^{1–3} it consists of 48 braided wires with approximately 30%–35% metal coverage, which disrupts the intra-aneurysmal blood flow, leading to aneurysmal thrombosis.⁴ The device is extremely flexible when deployed and can theoretically fit the original anatomy with minimal anatomical deformation, regardless of the regional tortuosity.⁵

To date, the adverse effects of PED deployment on the surrounding vascular structures are unknown. Previous reports have shown that the deployment of neck-bridging stents can sometimes cause parent artery straightening, which changes the vascular geometry, leading to thrombosis of the aneurysm by decreasing flow velocity toward the aneurysm.⁴ Although straightening of the

parent artery by stent deployment has beneficial effects on the progression of aneurysmal thrombosis, it simultaneously carries the potential risk of complications.⁶

Herein, we report a case of PED deployment for a large posterior communicating artery aneurysm, which changed the vascular geometry and hemodynamic stress of the adjacent ipsilateral anterior choroidal artery aneurysm, leading to aneurysmal rupture 3 years later. We further sought to elucidate the mechanism underlying this negative outcome using flow dynamics analysis.

Illustrative Case

A 71-year-old woman, incidentally found to have multiple aneurysms during an investigation for headache, was admitted to our

ABBREVIATIONS DSA = digital subtraction angiography; ICA = internal carotid artery; MAFA = mean aneurysm flow amplitude; PED = Pipeline embolization device.

INCLUDE WHEN CITING Published April 4, 2022; DOI: 10.3171/CASE21651.

SUBMITTED November 16, 2021. **ACCEPTED** February 15, 2022.

© 2022 The authors, CC BY-NC-ND 4.0 (<http://creativecommons.org/licenses/by-nc-nd/4.0/>).



FIG. 1. DSA of the left ICA. **A:** Initial DSA shows the coexistence of a large posterior communicating artery aneurysm (*arrowhead*) and a small anterior choroidal artery aneurysm (*arrow*). **B:** DSA and cone-beam computed tomography immediately after PED deployment. Although we initially deployed a PED from the bifurcation of the left ICA, the distal end of the stent slipped down during the procedure (*arrows*). Note that the PED barely covers the neck of the anterior choroidal artery aneurysm. **C:** DSA and cone-beam computed tomography at 6 months after endovascular therapy. Complete obliteration of the posterior communicating artery aneurysm in contrast to the residual anterior choroidal artery aneurysm can be observed; note the distal shortening of the PED leading to the exposure of the anterior choroidal aneurysm to the parent artery (*arrows*). **D:** DSA after the onset of subarachnoid hemorrhage. The anterior choroidal artery aneurysm is slightly enlarged and accompanied by the formation of a new bleb.

hospital. Preoperative digital subtraction angiography (DSA) showed a large posterior communicating artery aneurysm (maximum size, 12.7 mm) in addition to an ipsilateral small anterior choroidal artery aneurysm (maximum size, 2.6 mm) (Figs. 1A and 2A). Because the two aneurysms were close to each other in the left internal carotid artery (ICA), we planned to treat both aneurysms simultaneously using a PED. The patient received oral antiplatelet drugs (aspirin 100 mg and clopidogrel 75 mg) preoperatively and intravenous heparin during the procedure to maintain the activated coagulation time in the range of 250–300 seconds. With the patient under general anesthesia, both the 8-French Roadmaster TH catheter (Goodman) and 5-French Cerulean G catheter were placed in parallel in the left ICA via a femoral artery access. After a 5-French Navien catheter (Medtronic-Covidien) was parked at the cavernous portion of the left ICA through the 8-French Roadmaster catheter, a Marksman microcatheter (Medtronic-Covidien) was introduced into the left middle cerebral artery. Subsequently, an SL-10 microcatheter (Stryker Neurovascular) was navigated into the posterior communicating

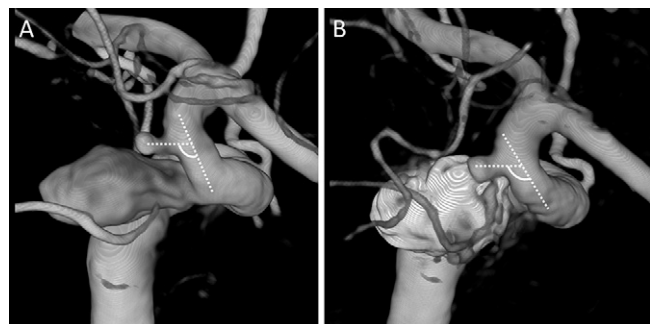


FIG. 2. Three-dimensional DSA (3D-DSA) of the left ICA. **A:** Preoperative image showing bending of the left ICA juxtaposed to the anterior choroidal artery aneurysm. The flow angle of the anterior choroidal artery aneurysm is 100°. **B:** 3D-DSA at 6 months after PED deployment. Distal shortening of the PED resulting in the uncovering of the anterior choroidal artery aneurysm. The flow angle of the anterior choroidal artery aneurysm changes from 100° to 125°.

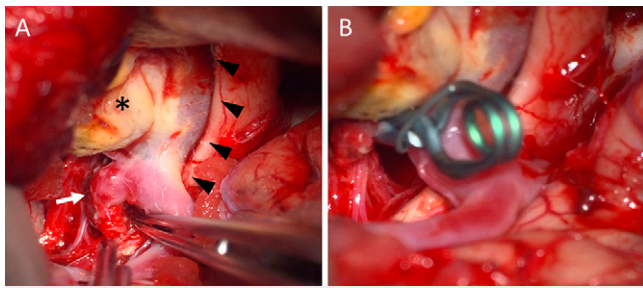


FIG. 3. Intraoperative findings of the surgical clipping. **A:** Anterior choroidal artery aneurysm is covered with a fibrin cap, indicating its rupture. Note the thrombosed posterior choroidal artery aneurysm (asterisk) and transparently visualized PED (arrowheads) inside the left ICA proximal to the anterior choroidal artery aneurysm. **B:** The ruptured anterior choroidal artery aneurysm was surgically clipped, and the anterior choroidal artery was preserved.

artery aneurysm through the 5-French Cerulean G catheter. Although we attempted to deploy a PED (4.25 mm × 16 mm) from the bifurcation of the left ICA, the distal end of the stent unexpectedly slid down during the procedure, which barely covered the neck of the anterior choroidal artery aneurysm. After the PED deployment, coil embolization of the posterior communicating artery aneurysm was performed through the SL-10 microcatheter using the jailing technique. Because cone-beam computed tomography after the PED deployment and the SL-10 microcatheter removal revealed good wall apposition of the stent, balloon plasty was not performed. Both aneurysms were initially covered with the PED, whereas the straightening of the left ICA due to the PED became prominent (Fig. 1B).

Follow-up DSA was performed 6 months after the endovascular therapy, revealing complete occlusion of the posterior communicating

artery aneurysm with a remnant of the anterior choroidal artery aneurysm (Fig. 1C). Unexpectedly, distal shortening of the PED occurred, leading to the exposure of the anterior choroidal artery aneurysm to the parent artery (Fig. 1C). Although the flow angle of the anterior choroidal artery aneurysm was 100° before PED deployment (Fig. 2A), it changed to 125° at 6 months after the endovascular therapy (Fig. 2B). Because the anterior choroidal artery aneurysm was small, we decided not to perform additional treatment and to continue with the angiographic follow-up.

Three years after the endovascular therapy, the patient was admitted to our hospital with a sudden onset of severe headache. On admission, her Glasgow Coma Scale score was 13 (eyes, 3; verbal, 4; motor, 6) without focal neurological signs. Because computed tomography showed diffuse subarachnoid hemorrhage, emergent DSA was performed, which showed no recurrence of the posterior communicating artery aneurysm. In contrast, the anterior choroidal artery aneurysm was slightly enlarged and accompanied by the formation of a new bleb (Fig. 1D), suggesting that the anterior choroidal artery aneurysm was responsible for the onset of the subarachnoid hemorrhage. She underwent surgical clipping for the anterior choroidal artery aneurysm by the left pterional approach. Intraoperative findings revealed that the anterior choroidal artery aneurysm was covered with a fibrin cap (Fig. 3A), indicating rupture. Complete clipping was achieved with preservation of the anterior choroidal artery (Fig. 3B). The patient's postoperative course was uneventful, and she was discharged to a rehabilitation hospital with a modified Rankin scale score of 3.

We retrospectively analyzed the hemodynamic changes in the anterior choroidal artery aneurysm before and after PED deployment using the flow analysis software on the Philips Healthcare interventional workstation (AneurysmFlow, XtraVision workstation release 8.8.1, Philips Healthcare) (Fig. 4). By applying an optical

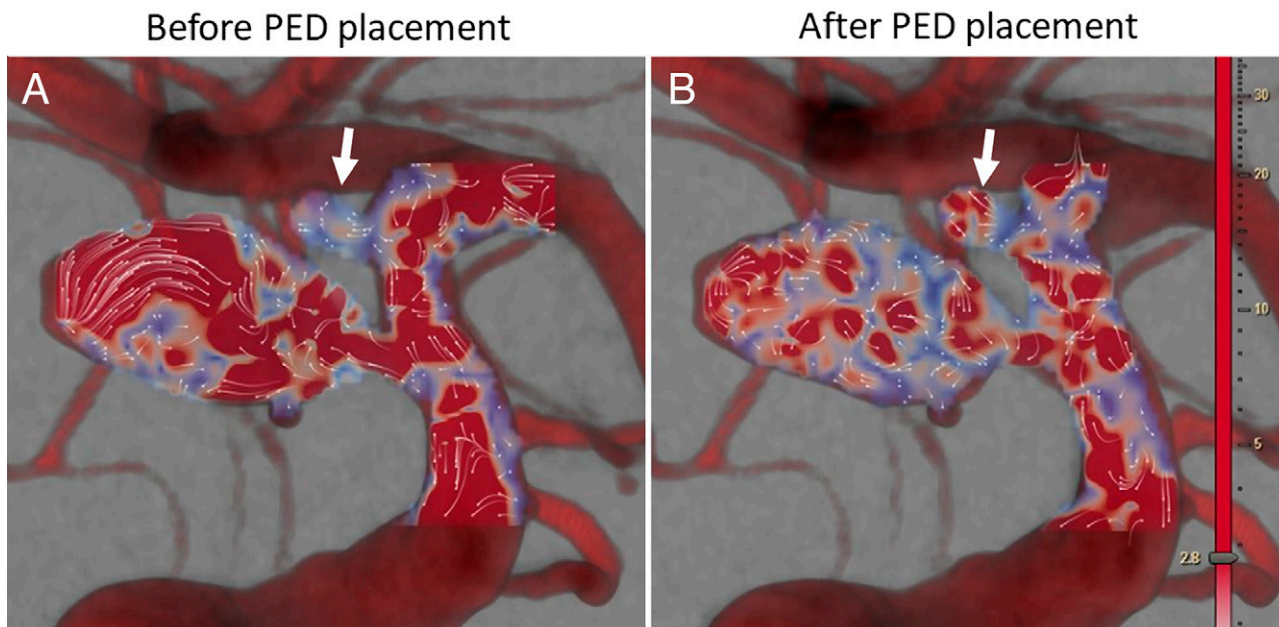


FIG. 4. Hemodynamics of the anterior choroidal artery aneurysm before (A) and after (B) the PED deployment. Aneurysm flow amplitude displaying averaged detector velocity fields (white dots with lines showing the direction of travel) superimposed on a velocity magnitude color map (m^2/s ; blue = slower, red = faster). After PED deployment, the MAFA significantly increased inside the anterior choroidal artery aneurysm (arrows), whereas the flow amplitude in the posterior communicating artery aneurysm decreased.

flow algorithm to the DSA time series, the software determined the flow within the aneurysm sac and automatically calculated the mean aneurysm flow amplitude (MAFA) ratio.^{7,8} The MAFA value of the left anterior choroidal artery aneurysm increased from 0.43 ml/s to 0.68 ml/s after the PED deployment, and the ratio of the increase in MAFA was calculated to be 1.54.

Discussion

Observations

The effects of PED deployment on the surrounding vascular structure have not been clarified thus far. According to previous reports, neck-bridging stents promote aneurysmal thrombosis by the straightening effect.^{5,9} On the one hand, computational fluid dynamics analysis shows that the change in the angle of the parent vessel after stent deployment reduces the blood flow into the aneurysm, leading to aneurysmal thrombosis.^{5,9,10} On the other hand, the stent-induced straightening of the surrounding vascular structure carries the risk of potential complications.⁵ Straightening of the parent artery by the neck-bridging stent has been reported to induce kinking of the distal portion, resulting in an unexpected occlusion of the vessel. In the present case, the supraclinoid portion of the left ICA straightened after PED deployment, although the straightening effect after PED deployment has not been reported previously. Because the straightening of the surrounding vascular structure carries a risk of complications, we should pay attention to the geometrical changes occurring after PED deployment.

The interesting finding of the present case is the delayed change in stent coverage at the distal end of the PED, resulting in the failure of the anterior choroidal artery aneurysm. This unfavorable situation could have been caused by either PED shortening or migration. A previous study reported that the prevalence rate of delayed PED shortening or migration ranged from 2.2% to 4.9%.¹¹ The mechanism of delayed stent shortening is called the “accordion effect,” whereas that of the delayed stent migration is termed the “watermelon seed” effect.^{12,13} The accordion effect is the phenomenon of foreshortening of a device that can be stretched forcibly during stent opening.^{12,13} In contrast, the watermelon seed effect is a phenomenon of proximal device migration when there is a significant difference in diameter between the proximal and distal vessels.^{11,13} In the present case, there was no significant difference in luminal diameter between the inflow and outflow vessels, and the proximal end of the PED did not move at all after stent deployment. Therefore, we think that the accordion effect was mainly responsible for the delayed change in stent coverage. The choice of small PED might have resulted in foreshortening of the stent in the present case. In addition, considering the possibility of foreshortening of the stent, PED should be deployed from M1. Taken together, avoiding stretching the PED during deployment, proper placement of the stent, and using a longer and appropriate-sized PED to adequately cover the targeted aneurysms might prevent the adverse outcome caused by the accordion effect.

Another interesting finding of the present case is that PED deployment changes the vascular geometry and aneurysm hemodynamics of the adjacent cerebral aneurysm. Follow-up DSA revealed that the flow angle of the anterior choroidal artery aneurysm and the relationship of the aneurysm dome to the parent artery¹⁴ significantly increased due to the straightening effect of the PED. A previous report showed that increasing the flow angle would lead to a deeper migration of the flow recirculation zone into the aneurysm,

resulting in a higher inflow velocity and wall shear stress in both the inflow zone and dome, thus causing rupture.¹⁵ Indeed, the flow velocity inside the anterior choroidal artery aneurysm, calculated as MAFA using the flow analysis software, revealed a dramatic increase after PED deployment, which probably promoted subsequent rupture in our case. Based on these findings, after endovascular therapy, management should be undertaken with great caution if the flow angle increases in the adjacent aneurysm due to incomplete PED placement. If the flow analysis suggests a substantial risk of rupture in the adjacent aneurysm, aggressive treatment, including second PED deployment, should be considered, even if the aneurysm is small.

Lessons

Because PED might induce the adverse effects on the adjacent uncovered aneurysm by changing the vascular geometry as well as hemodynamic stress, a cautious therapeutic strategy, such as proper placement of the stent and using a longer and appropriate-sized PED, should be adopted when deploying the PED. In addition, aggressive treatment should be considered if flow analysis reveals an increased risk of rupture.

Acknowledgments

We thank Hirotaka Sato for assistance with the figures. This work was supported by Japan Society for the Promotion of Science (JSPS) KAKENHI (grant JP19K18414 to H.S.).

References

1. Fiorella D, Lylyk P, Szikora I, et al. Curative cerebrovascular reconstruction with the Pipeline embolization device: the emergence of definitive endovascular therapy for intracranial aneurysms. *J Neurointerv Surg*. 2018;10(suppl 1):i9-i18.
2. Brinjikji W, Murad MH, Lanzino G, Cloft HJ, Kallmes DF. Endovascular treatment of intracranial aneurysms with flow diverters: a meta-analysis. *Stroke*. 2013;44(2):442-447.
3. Kallmes DF, Hanel R, Lopes D, et al. International retrospective study of the Pipeline embolization device: a multicenter aneurysm treatment study. *AJNR Am J Neuroradiol*. 2015;36(1):108-115.
4. D'Urso PI, Lanzino G, Cloft HJ, Kallmes DF. Flow diversion for intracranial aneurysms: a review. *Stroke*. 2011;42(8):2363-2368.
5. Gao B, Baharoglu MI, Malek AM. Angular remodeling in single stent-assisted coiling displaces and attenuates the flow impingement zone at the neck of intracranial bifurcation aneurysms. *Neurosurgery*. 2013;72(5):739-748.
6. Kono K, Shintani A, Tanaka Y, Terada T. Delayed in-stent occlusion due to stent-related changes in vascular geometry after cerebral aneurysm treatment. *Neurol Med Chir (Tokyo)*. 2013;53(3):182-185.
7. Pereira VM, Bonnefous O, Ouared R, et al. A DSA-based method using contrast-motion estimation for the assessment of the intra-aneurysmal flow changes induced by flow-diverter stents. *AJNR Am J Neuroradiol*. 2013;34(4):808-815.
8. Cancelliere NM, Nicholson P, Radovanovic I, et al. Comparison of intra-aneurysmal flow modification using optical flow imaging to evaluate the performance of Evolve and Pipeline flow diverting stents. *J Neurointerv Surg*. 2020;12(8):814-817.
9. Takemoto K, Tateshima S, Rastogi S, et al. Disappearance of a small intracranial aneurysm as a result of vessel straightening and in-stent stenosis following use of an Enterprise vascular reconstruction device. *J Neurointerv Surg*. 2014;6(1):e4.
10. Gao B, Baharoglu MI, Cohen AD, Malek AM. Y-stent coiling of basilar bifurcation aneurysms induces a dynamic angular vascular

remodeling with alteration of the apical wall shear stress pattern. *Neurosurgery*. 2013;72(4):617–629.

11. Tsai YH, Wong HF, Hsu SW. Endovascular management of spontaneous delayed migration of the flow-diverter stent. *J Neuroradiol*. 2020;47(1):38–45.
12. Chalouhi N, Tjoumakaris SI, Gonzalez LF, et al. Spontaneous delayed migration/shortening of the Pipeline embolization device: report of 5 cases. *AJNR Am J Neuroradiol*. 2013;34(12):2326–2330.
13. Tsutsumi M, Kazekawa K, Onizuka M, et al. Accordion effect during carotid artery stenting: report of two cases and review of the literature. *Neuroradiology*. 2007;49(7):567–570.
14. Duan Z, Li Y, Guan S, et al. Morphological parameters and anatomical locations associated with rupture status of small intracranial aneurysms. *Sci Rep*. 2018;8(1):6440.
15. Weir B, Disney L, Karrison T. Sizes of ruptured and unruptured aneurysms in relation to their sites and the ages of patients. *J Neurosurg*. 2002;96(1):64–70.

Disclosures

The authors report no conflict of interest concerning the materials or methods used in this study or the findings specified in this paper.

Author Contributions

Conception and design: Sakata, Nakayashiki, Ezura, Endo, Inoue. Acquisition of data: Sakata, Ezura, Endo. Analysis and interpretation of data: Sakata, Endo. Drafting the article: Sakata. Critically revising the article: Sakata, Endo. Reviewed submitted version of manuscript: Sakata, Ezura, Endo. Approved the final version of the manuscript on behalf of all authors: Sakata. Administrative/technical/material support: Saito. Study supervision: Ezura, Inoue, Saito, Tominaga.

Correspondence

Hiroyuki Sakata: National Hospital Organization Sendai Medical Center, Miyagi, Japan. sakata@nsg.med.tohoku.ac.jp.